

# Rapid Elastic Architecture Search under Specialized Classes and Resource Constraints

Jing Liu<sup>1</sup>, Bohan Zhuang<sup>1†</sup>, Mingkui Tan<sup>2†</sup>, Xu Liu<sup>2</sup>,  
Dinh Phung<sup>1</sup>, Yuanqing Li<sup>2</sup>, Jianfei Cai<sup>1</sup>

<sup>1</sup>Monash University <sup>2</sup>South China University of Technology

## Abstract

In many real-world applications, we often need to handle various deployment scenarios, where the resource constraint and the superclass of interest corresponding to a group of classes are dynamically specified. How to efficiently deploy deep models for diverse deployment scenarios is a new challenge. Previous NAS approaches seek to design architectures for all classes simultaneously, which may not be optimal for some individual superclasses. A straightforward solution is to search an architecture from scratch for each deployment scenario, which however is computation-intensive and impractical. To address this, we present a novel and general framework, called Elastic Architecture Search (EAS), permitting instant specializations at runtime for diverse superclasses with various resource constraints. To this end, we first propose to effectively train an over-parameterized network via a superclass dropout strategy during training. In this way, the resulting model is robust to the subsequent superclasses dropping at inference time. Based on the well-trained over-parameterized network, we then propose an efficient architecture generator to obtain promising architectures within a single forward pass. Experiments on three image classification datasets show that EAS is able to find more compact networks with better performance while remarkably being orders of magnitude faster than state-of-the-art NAS methods, e.g., outperforming OFA (once-for-all) by 1.3% on Top-1 accuracy at a budget around 361M #MAdds on ImageNet-10. More critically, EAS is able to find compact architectures within 0.1 second for 50 deployment scenarios.

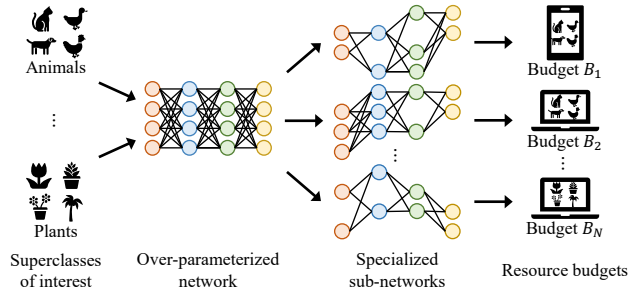


Figure 1. An illustration of model deployment for specified application scenarios, e.g., animal classification under various resource budgets. The optimal architectures shall be different for different deployment scenarios

flexible during deployment (e.g., focusing on classifying tens of classes), as shown in Figure 1. For example, zoologists might only be interested in classifying animals such as cat, dog, and so on, while many other classes provided by the general model might be useless to their tasks of interest. A usual additional requirement in practice is to deploy models to diverse platforms with different resource budgets (e.g., latency, energy, memory constraints). On the other hand, the computational budget varies due to the consumption of background apps that reduce the available computing capacity, and the energy budget varies due to the decreasing battery level of a mobile phone. These scenarios give rise to a new challenge: *how to instantly find an accurate and compact architectural configuration, given a specified superclass of interest and resource budget at runtime.*

To obtain compact architectures, most existing approaches either manually design [25, 59] or use model compression [45, 78, 79] and neural architecture search (NAS) [4, 7, 80] methods to find a specialized network. However, they are severely inflexible by a assumption that all the superclasses (each superclass corresponds to a group of classes) are predicted at the same time. In particular, for different superclass (e.g., animal and plant) classification tasks, the optimal architectures can differ significantly, making this assumption undesirable to search for optimal architectures tailored for different task requirements. Repeatedly retrain-

## 1. Introduction

Deep neural networks (DNNs) have achieved state-of-the-art performance in many areas in machine learning [21, 56] and much broader in artificial intelligence. There are numerous practical applications where we need a well-trained general model (capable of classifying thousands of classes) to be

<sup>†</sup>Corresponding author.

ing the network to find architectures for each superclass is extremely time-consuming and computation-intensive as the training cost grows linearly with the number of possible cases, and there are vast varieties of devices and dynamic deployment environments, which further exacerbate the efficiency problem significantly.

To address the above issue, one may consider the one-shot NAS methods to decouple the model training and the architecture search stage, where different sub-networks can be extracted from a well-trained over-parameterized network without any retraining [3, 73]. However, existing methods suffer from two limitations. First, there exists a gap between training and deployment since the over-parameterized network is trained on all superclass data while specialized sub-networks focus on some specific superclasses. Second, existing one-shot NAS methods learn a surrogate model to estimate the model accuracy of the architecture and then use evolutionary algorithm [3] or coarse-to-fine strategy [73] to find optimal architectures during the deployment stage. Nevertheless, training a surrogate model requires plenty of architectures with the ground-truth accuracy which are time-consuming to collect (*e.g.*, 40 GPU hours to collect 16K sub-networks in OFA [3]). Moreover, for  $M$  requirements of different superclasses with diverse resources, existing methods have to search  $M$  times, which takes unbearable computational cost.

To tackle these challenges, in this paper, we introduce a novel and general framework, called Elastic Architecture Search (EAS), to deliver instant and effective trade-offs between accuracy and efficiency to support diverse superclasses of interest under different hardware constraints. Specifically, the proposed EAS trains an over-parameterized network that supports many sub-networks and generates the architectures on the fly according to arbitrary deploying scenarios. To this end, we propose a superclass dropout strategy that randomly drops the output logits corresponding to different superclasses during training. In this way, we enforce the over-parameterized network to pay more attention to the target superclass. As a result, the over-parameterized network is robust to the superclass specification at testing time. To enable specializations to arbitrary superclasses with different resources, we further propose an architecture generator to obtain architectures within a single forward pass, which is extremely efficient.

Our main contributions are summarized as follows:

- We study a novel practical deep model deployment task for diverse superclasses of interest with arbitrary hardware resources, which has not been well studied. To resolve this, we devise a novel framework, called Elastic Architecture Search (EAS), which supports versatile architectures for various deployment requirements at runtime.
- We propose a superclass dropout strategy to pay more

attention to the target superclass during training, making the over-parameterized network robust to the subsequent superclass specification during deployment. We further design an architecture generator to generate architectures without the need to search from scratch for each scenario, which greatly reduces the specialization cost.

- Experiments on three image classification datasets show the superior performance and efficiency of the proposed EAS. For example, our EAS surpasses OFA by 1.3% in Top-1 accuracy at the budget level of 361M #MAdds on ImageNet-10. More impressively, our proposed EAS is able to find accurate and compact architectures within 0.1 second for 50 deployment scenarios.

## 2. Related work

**Network compression.** Network compression aims to reduce the model size and speed up the inference without significantly deteriorating the model performance. Existing network compression methods can be divided into several categories, including but not limited to network pruning [16, 38, 40, 45], network quantization [13, 34, 77, 78], knowledge distillation [22, 47, 57, 75], low-rank decomposition [11, 28, 48, 74], *etc.* Although achieving promising performance, prevailing methods only target predicting all the classes simultaneously. For different groups of classes, it requires repeatedly retraining to find a compact network for each group, which is time-consuming and inefficient. In contrast, our proposed EAS trains an over-parameterized network that supports a great number of sub-networks for diverse superclasses with different resources.

**Neural architecture search (NAS).** NAS seeks to design efficient architectures automatically instead of relying on human expertise. Existing NAS methods can be roughly divided into three categories according to the search strategy, namely, reinforcement learning-based methods [18, 49, 63, 80], evolutionary methods [42, 43, 52, 53], and gradient-based methods [4, 27, 37, 68]. To efficiently explore the enormous search space, existing gradient-based multi-path NAS methods [27, 68] relax the search space to be continuous and formulate the optimization as a path selection problem. Compared with these methods, our method transforms the NAS problem into a subset selection problem following single-path NAS [60, 61], which significantly reduces the number of parameters and computational cost.

When it comes to different resource constraints, existing methods have to repeatedly retrain the network and search for optimal architectures. To solve this, one-shot NAS methods [3, 20, 73] have been proposed to train a once-for-all network that supports different architectural configurations by decoupling the model training stage and the architecture search stage. To search for optimal architectures efficiently, one can use evolutionary search [3] or design an architecture

generator to obtain effective architectures [58, 71]. However, given different resource constraints, these methods have to search architectures for each deployment scenario, which is inefficient. Unlike these methods, we propose an efficient architecture generator that is able to obtain architectures on the fly within one forward pass given diverse superclasses with different resource constraints.

**Dynamic neural networks.** Dynamic neural networks, as opposed to static ones, are able to adapt their structures or parameters to different inputs during inference and therefore enjoy the desired trade-off between accuracy and efficiency. Existing methods can be roughly divided into three categories according to the granularity of dynamic networks, namely, instance-wise [8, 26, 36, 66], spatial-wise [54, 55, 67] and temporal-wise dynamic networks [15, 69, 70]. However, the inference efficiency of the data-dependent dynamic networks relies on the largest activated network in a batch of data, which limits the degree of practicality. Moreover, all the above methods perform predictions on all superclasses simultaneously. Unlike these methods, our proposed EAS is able to derive compact and accurate architectures given arbitrary superclasses and efficiency constraints.

**Multi-task learning.** Multi-task learning takes advantage of useful information contained in multiple related tasks to improve the performance of the learned models on all tasks. Existing methods can be roughly divided into several categories, including but not limited to feature learning approaches [39, 76], low-rank methods [1, 6], task clustering approaches [9, 64], task relation learning methods [14, 46], decomposition approaches [5, 29], *etc.* Recently, several methods are proposed for architecture design [62] or fast specialization [31] under a limited number of budgets for multi-task learning. Unlike these methods, our proposed method focuses on fast architecture specializations with elastic depth, width expansion ratio, and kernel size for diverse tasks under various resource budgets during deployment. More critically, most multi-task learning methods can be easily applied on top of our proposed method. For example, we can apply multi-task learning methods during the training of the over-parameterized network to improve the performance of all superclasses.

### 3. Elastic architecture search

**Notation.** Let  $\mathcal{D}^t = \{(\mathbf{x}_n^t, y_n^t)\}_{n=1}^{N^t}$  be the training data for  $t$ -th superclass, where  $\mathbf{x}_n^t \in \mathcal{X}^t$ ,  $y_n^t \in \mathcal{Y}^t$ , and  $N^t$  is the number of images. For simplicity, different superclasses of data are disjoint and focus on different classes, namely,  $\forall i, j \in \{1, \dots, T\}$  and  $i \neq j$ ,  $\mathcal{Y}^i \cap \mathcal{Y}^j = \emptyset$ , and  $D^i \cap D^j = \emptyset$ . Let  $\mathcal{D} = \{(\mathbf{x}_n, y_n)\}_{n=1}^N = \cup_{t=1}^T \mathcal{D}^t$  be the union of data for  $T$  superclasses, where  $N = \sum_{t=1}^T N^t$ .

In this paper, we focus on elastic architecture search problem that aims to obtain architectures given arbitrary superclasses with different resource budgets. To address this, one

may use existing NAS methods [4, 49] to search architectures for each superclass and resource budget. However, when it comes to a vast amount of superclasses with various resource requirements, designing a specialized network for every scenario is computationally expensive and impractical.

To handle diverse superclasses with different resource budgets dynamically during testing, we propose a novel method, called Elastic Architecture Search (EAS). Specifically, our proposed EAS trains an over-parameterized network on  $\mathcal{D}$  that supports a very large number of sub-networks. However, the training of the over-parameterized network is a highly entangled bi-level optimization problem [37]. Inspired by one-shot NAS [3, 20, 73], our solution is to decouple the model training stage and the architecture search stage. To make the model robust to the subsequent superclass specification during inference, we present a superclass dropout strategy at training time (See Section 3.1). Once the over-parameterized network has been well-trained, we are able to search architectures for different superclasses under various resources without any retraining. In particular, we propose an efficient architecture generator to obtain optimal architectures within one forward pass (See Section 3.2).

#### 3.1. Superclass Dropout

Following [3], the over-parameterized network consists of many sub-networks with different depths, width expansion ratios, and kernel sizes, where the weights of small sub-networks are shared with large sub-networks. To prevent interference between different sub-networks, we use the progressive shrinking strategy to train the over-parameterized network following [3]. However, existing methods ignore the gap between the training and deployment where the over-parameterized network is trained on all superclass data while the specialized networks only concentrate on some specific superclasses. To mitigate the gap, one may train an over-parameterized network for each  $\mathcal{D}^t$  separately, which is computationally expensive and impractical. Such method also ignores that the data from other superclasses may contain useful context information for the target superclass, which may result in sub-optimal performance of the sub-networks.

To resolve these issues, motivated by [23, 65], we propose to train an over-parameterized network on  $\mathcal{D}$  with the superclass dropout strategy that randomly drops the output logits corresponding to non-target superclasses at each step of optimization, as shown in Figure 2a. Formally, let  $\mathbf{v}_n \in \mathbb{R}^d$  be the input feature of the last fully connected layer corresponding to  $\mathbf{x}_n$ , where  $d$  is the input feature dimension. For convenience, we omit the sample index  $n$ . The output logits of the network, denoted by  $\mathbf{o}$ , can be computed by  $\mathbf{o} = \mathbf{w}^\top \mathbf{v}$ , where  $\mathbf{w} \in \mathbb{R}^{d \times C}$  denotes the weights of the last fully connected layer and  $C$  is the number of classes. To encode the dropping decision of classes, we introduce a binary

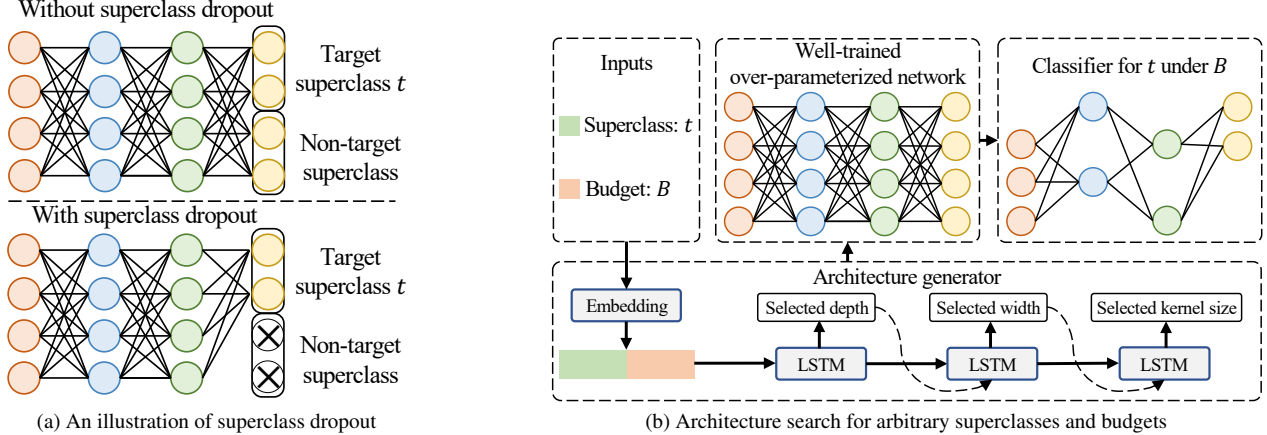


Figure 2. The overview of the superclass dropout and architecture search. (a) We apply superclass dropout which randomly drops the output logits corresponding to different superclasses during the training of the over-parameterized network. (b) We build an architecture generator, which takes a superclass label  $t$  and resource budget  $B$  as inputs and generates architectures that satisfy the requirement. We use an embedding layer to map the superclass label and budget to the concatenated embedding vector

mask  $\mathbf{m} \in \{0, 1\}^C$  to the output logits of the network:

$$\hat{\mathbf{o}} = \mathbf{m} \odot \mathbf{o}, \quad (1)$$

where  $\odot$  is an operation of the element-wise product and  $\hat{\mathbf{o}}$  is the masked version of  $\mathbf{o}$ . Without any constraint, Eq. (1) is a form of class dropping. To enable superclass dropping, the binary mask  $\mathbf{m}$  must be organized into groups by  $\mathcal{G} = \{G^1, \dots, G^T\}$ , where  $\cup_{t=1}^T G^t = \{1, \dots, C\}$ ,  $G^i \cap G^j = \emptyset$  for  $\forall i, j$  and  $i \neq j$ , and  $G^t$  denotes the index set of binary mask belonging to the  $t$ -th group. In this case, the output logits of the  $t$ -th superclass are

$$\hat{\mathbf{o}}_{G^t} = \mathbf{m}_{G^t} \odot \mathbf{o}_{G^t}, \quad (2)$$

where  $\hat{\mathbf{o}}_{G^t}$ ,  $\mathbf{m}_{G^t}$  and  $\mathbf{o}_{G^t}$  are the  $t$ -th group components of  $\hat{\mathbf{o}}$ ,  $\mathbf{m}$  and  $\mathbf{o}$ , respectively. Here, the binary mask  $\mathbf{m}_{G^t}$  controls the dropping decision of the superclass  $t$ . During the model training stage, for any sample  $(\mathbf{x}^t, y^t) \in \mathcal{D}^t$  in a batch of data, the binary mask  $\mathbf{m}_{G^t}$  corresponding to a non-target superclass  $j$  (i.e.,  $\forall j \in \{1, \dots, T\}$  and  $j \neq t$ ) is randomly set to zero following a Bernoulli distribution with a hyper-parameter  $q \in [0, 1]$  that controls the drop rate, while the binary mask corresponding to the target superclass  $t$  is set to one. Then, we compute the output probabilities using non-zero elements in  $\hat{\mathbf{o}}_{G^t}$ . In this way, we enforce the over-parameterized network to pay more attention to the target superclass in each update step during training. As a consequence, the sub-networks derived from the over-parameterized network are more robust to superclass dropping during deployment.

### 3.2. Architecture Generator

Once the over-parameterized network has been well-trained, we now focus on how to quickly find specialized

sub-networks from the over-parameterized network given arbitrary deployment scenarios. To find optimal architectures, one may train a surrogate model to learn the mapping from an architectural configuration to its accuracy and then use the evolutionary algorithm [3] or coarse-to-fine strategy [73] to explore the large configuration space. However, training such a surrogate model requires plenty of architecture-accuracy pairs that are very expensive to obtain in practice (e.g., 40 GPU hours to collect 16K sub-networks in OFA [3]). Moreover, for different superclasses with various resource budgets, existing methods have to search architectures for each deployment scenario, which is extremely inefficient and unnecessary.

To solve the above issue, we propose an architecture generator model to obtain architectures for diverse superclasses with different resources within a single forward pass. As shown in Figure 2b, the architecture generator  $G(B, t; \theta)$  is based on an LSTM network with three fully connected layers to predict the depth, width and kernel size configurations following [49]. Here,  $\theta$  is the parameters of the architecture generator. Specifically,  $G(B, t; \theta)$  takes a resource budget  $B$  and superclass label  $t$  as inputs and generates the architecture encoding  $\alpha$ . Following [19, 49], we define  $K$  budgets evenly sampled from the range of  $[B_L, B_H]$ , where  $B_L$  and  $B_H$  are the minimum and maximum of resource budgets, respectively. To represent different superclasses and budgets, we build learnable embedding vectors for each of the superclass labels and predefined budgets. To deal with a resource budget with an arbitrary value, we use an embedding interpolation method following [17, 51]. We then concatenate the resulting budget and superclass embedding vectors and feed them into the LSTM network. By incorporating the learnable embedding vectors into the parameters of the architecture

---

**Algorithm 1** Training method for the architecture generator.

---

**Require:** The parameters of the well-trained over-parameterized network  $\mathbf{W}$ , minimum of the resource budget  $B_L$ , maximum of the resource budget  $B_H$ , uniform distribution  $U(B_L, B_H)$ , total superclass number  $T$ , superclass index set  $\{1, \dots, T\}$ , learning rate  $\eta$ , training data set  $D = \cup_{t=1}^T \mathcal{D}^t$ , hyper-parameters  $\lambda$  and  $\tau$ .

- 1: Initialize the architecture generator parameters  $\theta$ .
  - 2: **while** not converged **do**
  - 3:   Randomly select a superclass label  $t$  from  $\{1, \dots, T\}$ .
  - 4:   Sample a batch of data from  $\mathcal{D}^t$ .
  - 5:   Sample a resource budget  $B$  from  $U(B_L, B_H)$ .
  - 6:   Compute the loss using Eq. (4).
  - 7:   Update the architecture generator by
  - 8:      $\theta \leftarrow \theta - \eta \nabla_{\theta} \mathcal{L}(\theta)$ .
  - 9: **end while**
- 

generator, we are able to train them jointly. The training details of the proposed architecture generator are shown in Algorithm 1.

**Objective function.** The goal of the architecture generator is to obtain an architecture encoding  $\alpha$  corresponding to a sub-network of the well-trained over-parameterized network that minimizes the validation loss  $\mathcal{L}_{\text{val}}(\mathbf{W}, \alpha)$ , where  $\mathbf{W}$  is the weights of the over-parameterized network. Here, the validation loss is the cross-entropy on the validation set. To ensure that the computational cost  $R(\alpha)$  is close to  $B$ , we introduce a computational constraint loss, which can be formulated as

$$\mathcal{L}_C(\alpha, B) = (R(\alpha) - B)^2. \quad (3)$$

By considering both the validation loss and computational constraint loss, the joint loss function can be formulated as

$$\mathcal{L}(\theta) = \mathcal{L}_{\text{val}}(\mathbf{W}, G(B, t; \theta)) + \lambda \mathcal{L}_C(G(B, t; \theta), B), \quad (4)$$

where  $\lambda$  is a hyper-parameter that balances two loss terms.

**Single-path architecture encoding.** Finding a sub-network from the well-trained over-parameterized network is a discrete and non-differentiable process. To address this, we propose to use single-path framework to encode architectural configurations (*i.e.*, kernel size, width expansion ratio) in the search space of the well-trained over-parameterized network and formulate the NAS problem as a subset selection problem. In this case, the architecture encoding  $\alpha$  can be represented by a series of binary gates that determine which subset of weights to use and the computational cost  $R(\alpha)$  is a function of the binary gates.

To encode kernel size and width expansion ratio configurations, we use the architecture encoding following single-path NAS [61]. Motivated by this, we also propose to encode the depth configurations in a single-path scheme. Specifically, a shallower network can be viewed as a subset of layers of the whole network. Thus, the depth configuration

can also be determined by a set of binary gates. Formally, let  $\mathcal{H}^l(\mathbf{x})$  be the mapping until the  $l$ -th module and  $\mathcal{F}(\cdot)$  be the mapping of the  $(l+1)$ -th module. Note that a module can be a layer or a block that consists of a collection of successive layers. Then, the mapping  $\mathcal{H}^{l+1}(\mathbf{x})$  until the  $(l+1)$ -th module can be formulated as

$$\mathcal{H}^{l+1}(\mathbf{x}) = \mathcal{H}^l(\mathbf{x}) \cdot (1 - g^{l+1}) + \mathcal{F}(\mathcal{H}^l(\mathbf{x})) \cdot g^{l+1}, \quad (5)$$

where  $g^{l+1}$  is a binary gate to determine whether to go through the  $(l+1)$ -th module during the forward propagation. In this case, the computational cost  $R^{l+1}$  until the  $(l+1)$ -th module is

$$R^{l+1} = R^l + r^{l+1} \cdot g^{l+1}, \quad (6)$$

where  $r^{l+1}$  is the computational cost of the  $(l+1)$ -th module.

Instead of determining the output of the binary gates using some heuristic metrics (*e.g.*, the  $\ell_1$ -norm of the weights), we force the output of each binary gate following the Bernoulli distribution with a probability  $p_i$ , where  $i$  denotes the index of the binary gate. Formally, the output of the  $i$ -th binary gate can be computed by

$$g(p_i) = \begin{cases} 1 & \text{with probability } p_i, \\ 0 & \text{with probability } 1 - p_i. \end{cases} \quad (7)$$

Therefore, the architecture encoding  $\alpha$  is encoded by a set of binary gates and each binary gate is sampled from the Bernoulli distribution. To obtain  $p_i$ , we apply a sigmoid function  $\sigma(\cdot)$  to the output  $\mathbf{z}$  of the LSTM network, which can be formulated as

$$p_i = \sigma(z_i), \quad (8)$$

where  $z_i$  is the  $i$ -th element of  $\mathbf{z}$ .

**Gumbel-Softmax for differentiable relaxation.** To train the architecture generator, we need to estimate the gradient of the objective function  $\mathcal{L}(\theta)$  w.r.t. the probability  $p_i$ . However, Eq. (7) is not differentiable w.r.t.  $p_i$ . Following [35], we use the Gumbel-Softmax reparameterization trick [30, 44] to reparameterize  $p_i$  as

$$h(p_i, \tau) = \sigma \left( \left( \log \frac{p_i}{1 - p_i} + \log \frac{u_i}{1 - u_i} \right) / \tau \right), \quad (9)$$

where  $u_i \sim U(0, 1)$  is the random noise sampled from the uniform distribution  $U(0, 1)$  and  $\tau$  is the temperature hyper-parameter. During the forward propagation, the output of a binary gate is computed by

$$\hat{g}(p_i) = \begin{cases} 1 & \text{if } h(p_i, \tau) > 0.5, \\ 0 & \text{otherwise,} \end{cases} \quad (10)$$

where  $\hat{g}(p_i)$  is the hard version of  $h(p_i, \tau)$ . During backward propagation, we use straight-through estimator (STE) [2, 77]

Table 1. Performance comparisons on ImageNet-10. We report the Top-1 Accuracy (Acc.) of different architectures on diverse superclasses. “Avg. Acc.” and “Avg. #MAdds” denote the average Top-1 accuracy and the average number of multiply-adds, respectively. A column of “T-t” shows the Top-1 accuracy on the t-th superclass. Different row sets report the Top-1 accuracy at different budget levels

Method	T-1	T-2	T-3	T-4	T-5	T-6	T-7	T-8	T-9	T-10	Avg. Acc. (%)	Avg. #MAdds (M)
OFA-V	86.7	90.7	79.7	81.0	85.0	<b>89.0</b>	82.0	96.0	92.7	<b>96.7</b>	87.9	230
OFA-T	86.3	90.0	79.7	79.0	85.3	87.3	<b>83.0</b>	<b>97.0</b>	93.3	<b>96.7</b>	87.8	230
EAS (Ours)	<b>89.0</b>	<b>91.3</b>	<b>81.7</b>	<b>81.3</b>	<b>86.7</b>	88.7	<b>83.0</b>	96.7	<b>94.0</b>	<b>96.7</b>	<b>88.9</b>	<b>219</b>
OFA-V	87.7	91.0	80.0	80.0	84.7	89.7	83.0	95.7	93.7	95.3	88.0	278
OFA-T	88.0	90.0	80.0	80.0	86.7	89.3	<b>85.0</b>	95.7	<b>94.3</b>	95.7	88.5	279
EAS (Ours)	<b>90.0</b>	<b>92.0</b>	<b>81.3</b>	<b>80.3</b>	<b>87.7</b>	<b>90.3</b>	84.3	<b>97.3</b>	<b>94.3</b>	<b>96.7</b>	<b>89.4</b>	<b>269</b>
OFA-V	88.3	90.7	81.0	79.7	85.7	<b>90.3</b>	83.7	95.0	92.7	<b>96.7</b>	88.4	329
OFA-T	88.0	90.0	80.0	80.3	86.0	90.0	<b>85.7</b>	95.7	93.7	95.7	88.5	328
EAS (Ours)	<b>89.3</b>	<b>91.7</b>	<b>82.0</b>	<b>82.3</b>	<b>89.0</b>	90.0	84.3	<b>97.3</b>	<b>94.3</b>	<b>96.7</b>	<b>89.7</b>	<b>316</b>
OFA-V	87.0	90.0	80.7	79.7	85.7	90.0	83.7	95.0	93.0	96.7	88.1	364
OFA-T	87.3	91.3	80.0	80.7	87.0	89.3	84.7	96.3	93.3	96.3	88.6	373
EAS (Ours)	<b>88.7</b>	<b>91.7</b>	<b>82.0</b>	<b>82.3</b>	<b>88.7</b>	<b>90.3</b>	<b>85.3</b>	<b>97.3</b>	<b>95.0</b>	<b>97.3</b>	<b>89.9</b>	<b>361</b>

Table 2. Performance comparisons on ImageNet-12. We report the Top-1 Accuracy (Acc.) of different architectures on diverse superclasses. “Avg. Acc.” and “Avg. #MAdds” denote the average Top-1 accuracy and the average number of multiply-adds, respectively. A column of “T-t” shows the Top-1 accuracy on the t-th superclass. Different row sets report the Top-1 accuracy at different budget levels

Method	T-1	T-2	T-3	T-4	T-5	T-6	T-7	T-8	T-9	T-10	T-11	T-12	Avg. Acc. (%)	Avg. #MAdds (M)
OFA-V	81.7	86.6	92.0	85.8	88.1	77.3	83.4	79.5	80.3	84.7	79.5	<b>79.4</b>	83.2	229
OFA-T	80.9	86.6	92.5	85.6	88.1	77.4	83.4	<b>79.6</b>	80.8	<b>85.2</b>	79.7	79.1	83.2	229
EAS (Ours)	<b>81.8</b>	<b>86.9</b>	<b>93.1</b>	<b>85.9</b>	<b>88.5</b>	<b>78.4</b>	<b>83.5</b>	<b>79.6</b>	<b>80.9</b>	84.7	<b>79.8</b>	78.1	<b>83.4</b>	<b>223</b>
OFA-V	<b>81.7</b>	87.0	92.8	<b>86.6</b>	87.8	78.0	83.7	78.9	81.6	84.9	<b>80.5</b>	78.6	83.5	278
OFA-T	81.1	87.0	92.6	86.2	<b>89.1</b>	<b>79.1</b>	<b>83.8</b>	<b>79.5</b>	81.3	85.2	80.2	78.5	83.6	279
EAS (Ours)	81.3	<b>87.4</b>	<b>92.9</b>	<b>86.6</b>	88.1	77.8	83.3	79.3	<b>81.9</b>	<b>85.5</b>	80.3	<b>80.0</b>	<b>83.7</b>	<b>266</b>
OFA-V	81.2	<b>87.9</b>	92.7	85.9	88.4	78.3	84.1	<b>79.5</b>	81.7	84.9	<b>80.8</b>	78.8	83.7	329
OFA-T	81.1	87.2	<b>93.0</b>	86.2	89.0	<b>79.3</b>	83.9	79.1	81.1	85.2	80.5	78.8	83.7	329
EAS (Ours)	<b>81.6</b>	87.5	<b>93.0</b>	<b>86.5</b>	<b>89.1</b>	78.6	<b>84.3</b>	79.3	<b>82.3</b>	<b>85.3</b>	80.1	<b>79.6</b>	<b>83.9</b>	<b>320</b>
OFA-V	81.0	87.2	92.8	85.9	88.5	78.3	84.4	<b>80.2</b>	81.5	85.0	<b>81.1</b>	78.7	83.7	379
OFA-T	80.8	87.3	<b>93.3</b>	85.9	89.0	<b>79.6</b>	<b>84.6</b>	79.9	81.7	85.4	80.0	79.0	83.9	379
EAS (Ours)	<b>81.5</b>	<b>87.7</b>	<b>93.3</b>	<b>86.8</b>	<b>89.4</b>	79.2	84.2	<b>80.2</b>	<b>82.0</b>	<b>86.0</b>	80.9	<b>79.9</b>	<b>84.3</b>	<b>358</b>

to approximate the gradient of  $\hat{g}(p_i)$  by the gradient of  $h(p_i, \tau)$ . In this way, the objective function  $\mathcal{L}(\theta)$  is differentiable w.r.t.  $p_i$ . Therefore, we are able to train the architecture generator using gradient-based methods.

**Inferring architectures for diverse superclasses with different resources.** Once the architecture generator has been well-trained, we can instantly search sub-networks that meet specified deployment scenarios. Specifically, given a superclass label and resource budget, the output of the architecture generator is the probabilities of the binary gates encoding the architectural configurations. Since we consider computational constraint loss during training, the architectures sampled from the learned distribution are expected to satisfy the computational constraint. We will repeat the sampling process if the sampled ones violate the resource budget. Last, we select the final architecture with the highest validation accuracy. Moreover, our architecture generator is able to generate architectures for  $M$  deployment requirements within a single forward pass by setting the mini-batch size to  $M$ .

## 4. Experiments

**Datasets.** We evaluate the proposed EAS on the large-scale image classification dataset, namely ImageNet [10]. We also evaluate our method on the fine-grained classification dataset Stanford Cars [33]. For each dataset, we construct superclasses by grouping semantically similar classes. Based on ImageNet, we construct two datasets following [12]. The first dataset, denoted by ImageNet-10, consists of 10 superclasses and each superclass contains 6 classes. The total number of training and testing samples for ImageNet-10 are 77,237 and 3,000, respectively. The second dataset, denoted by ImageNet-12, consists of 12 superclasses and each superclass contains 20 classes. The total number of training and testing samples for ImageNet-12 are 308,494 and 12,000, respectively. Based on Stanford Cars, we construct the third dataset, denoted by Car-20, which consists of 20 superclasses and each superclass contains 3 classes. The total number of training and testing samples are 2,494 and 2,463, respectively. For ImageNet-10 and ImageNet-12 datasets,

we randomly choose 10k training samples as the validation set. For Car-20 dataset, we randomly choose 500 training samples as the validation set. More details about the datasets are put in the supplementary material.

**Search space.** We apply our proposed EAS to MobileNetV3 [24] search space. Specifically, the model is split into 5 units following [3]. We choose the depth of each unit from  $\{2, 3, 4\}$ , the width expansion ratio of each inverted residual block from  $\{3, 4, 6\}$ , and the kernel size of each depthwise convolution from  $\{3, 5, 7\}$ .

**Compared methods.** We compare our EAS with the state-of-the-art one-shot NAS method OFA [3]. To perform classification on different superclasses, we construct the following variants for comparisons. **OFA-V**: the vanilla OFA that trains an over-parameterized network and only performs a single evolutionary search for all superclasses. **OFA-T**: trains an over-parameterized network and searches optimal architectures for each superclass.

**Evaluation metrics.** We measure the performance of different methods using the Top-1 accuracy on diverse superclasses given a specific budget. Following [24, 59], we measure the computational cost of the searched architectures using the number of multiply-adds (#MAdds). Following [37], we also use the training cost on a GPU device (GeForce RTX 3090) to measure the time of training an architecture generator and the search cost on a CPU device (Intel Xeon Gold 6230R) to measure the time of using the generator to find an optimal architecture.

**Implementation details.** We apply our proposed EAS to MobileNetV3 [24] search space following [3]. We first train an over-parameterized network on all superclasses of training data for 120 epochs using the progressive shrinking strategy [3] with a mini-batch size of 256. Different from OFA [3], we share the kernel weights among different kernel sizes without using the kernel transformation. We use SGD with a momentum of 0.9 for optimization [50]. The learning rate starts at 0.01 and decays with cosine annealing [41]. We set the drop rate  $q$  to 0.6, 0.1, and 0.15 for the experiments on ImageNet-10, ImageNet-12, and Car-20, respectively. We then train the architecture generator for 90 epochs on the validation set. The number of learnable embedding vectors  $K$  for the resource budget is set to 10. We set the dimension of the embedding vector to 32 for both the superclass label and resource budget. We use Adam for optimization [32] with a learning rate of  $1 \times 10^{-3}$ . The hyper-parameters  $\lambda$  and  $\tau$  are set to 0.01 and 1, respectively. For all experiments on ImageNet-10, ImageNet-12 and Car-20, we set  $B_L$  and  $B_H$  to 150 and 550, respectively. We put more implementation details in the supplementary material.

#### 4.1. Main Results

We show the results on ImageNet-10 and ImageNet-12 in Table 1 and Table 2, respectively. We also report the average

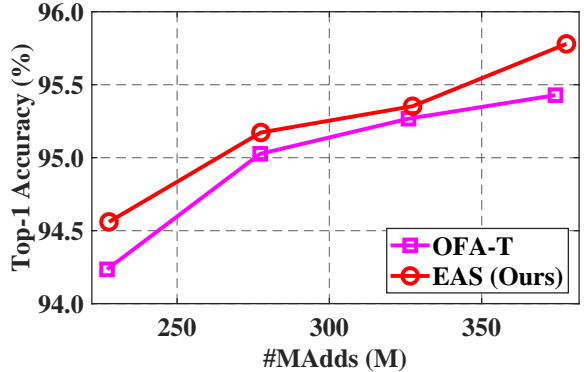


Figure 3. Performance comparisons of the proposed EAS with OFA-T under various budget levels on Car-20

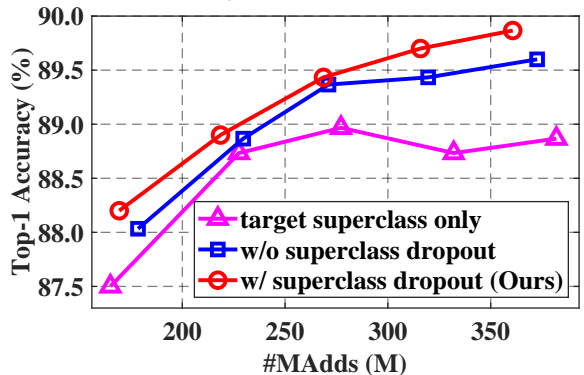


Figure 4. Performance comparisons of the proposed EAS with different superclass dropout strategies on ImageNet-10

Top-1 accuracy and average #MAdds across all superclasses of Car-20 in Figure 3. We put more results on Car-20 and visualization of the generated architectures in the supplementary material. Compared with OFA-V, OFA-T achieves better or comparable performance in all superclasses with different resource budgets. For example, on ImageNet-10, OFA-T surpasses OFA-V by 0.5% in terms of the average model accuracy at the resource budget level of 373M Avg. #MAdds. These results demonstrate that searching architectures for all superclasses may not be optimal for each superclass. Compared with OFA-T, our method achieves better or comparable model accuracy in all superclasses with diverse resource budgets. For the average performance of all superclasses on different resource budgets, our EAS consistently outperforms OFA-T by a large margin with fewer or comparable #MAdds. For example, on ImageNet-10, our EAS surpasses OFA-T by 1.3 % on the average Top-1 accuracy at the budget level of 361M Avg. #MAdds. These results verify the effectiveness of our method. Note that for superclass-2 of ImageNet-10, the obtained architecture of EAS achieves the best accuracy at the resource budget level of 269M Avg. #MAdds. With the increase of #MAdds, the accuracy of the searched architecture goes worse. Similar results are also observed for the baseline methods, such as

Table 3. Comparisons of the training time and search time for architecture search among different methods on ImageNet-10. The training time for OFA-T is the cost of sampling architecture-accuracy pairs and learning a surrogate model. For the multi-path AG and single-path AG, the training time is the cost of learning an architecture generator. The search time is the cost of finding architectures for 10 superclasses and 5 resource budgets

Method	OFA-T	Multi-path AG	Single-path AG (Ours)
Training Time (GPU hour)	104.0	<b>40.3</b>	<b>0.9</b>
Search Time (CPU second)	3474.1	<b>&lt;0.1</b>	<b>&lt;0.1</b>

superclass-7 of ImageNet-10 for OFA-T and superclass-1 of ImageNet-12 for OFA-V. One possible reason is that for those superclasses of data that are easy to be classified, using a compact network with low computational overhead is sufficient to obtain promising performance. Increasing the resource budget may suffer from the over-fitting issue.

## 4.2. Ablation Studies

**Effectiveness of the superclass dropout.** To investigate the effect of the superclass dropout strategy, we first train the over-parameterized networks with and without superclass dropout on ImageNet-10 and then use the proposed architecture generator to obtain architectures. We also train the over-parameterized network with the target superclass only by setting the drop rate  $q$  to 1, which indicates that we completely drop the output logits corresponding to the non-target superclasses during training. More results in terms of different drop rates are put in the supplementary material. We report the average Top-1 accuracy and average #MAdds across all superclasses in Figure 4. From the results, EAS without superclass dropout surpasses the one with the target superclass only, especially at high resource budget settings. These results verify that exploiting useful context information in other superclasses improves the performance of current superclass. More critically, EAS with superclass dropout consistently outperforms the one without superclass dropout and the performance improvement brought by the superclass dropout strategy is more significant at higher resource budget levels. For example, the architecture searched by the superclass dropout strategy yields a much lower average #MAdds (316M vs. 373M) but achieves better performance. These results demonstrate the effectiveness of the proposed superclass dropout strategy.

**Effectiveness of the architecture generator.** To investigate the effect of the architecture generator, we first train the over-parameterized network with superclass dropout on ImageNet-10 and then use the following methods to search for the architectures. 1) **Random**: randomly samples an architecture for each deployment scenario. 2) **OFA-T**: uses the evolutionary algorithm to search optimal architectures for diverse superclasses and resources [3]. 3) **Multi-path AG**: based on the proposed architecture generator, we use the multi-path scheme [37, 68] to encode the generated ar-

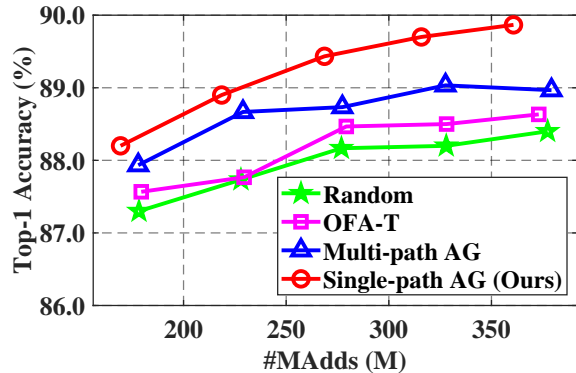


Figure 5. Performance comparisons of the proposed EAS with different search algorithms on ImageNet-10

chitectures for each superclass. 4) **Single-path AG**: uses the proposed architecture generator to obtain architectures with the single-path architecture encoding for each superclass. We report the average Top-1 accuracy and average #MAdds across all superclasses in Figure 5. We also show the training cost and search cost in Table 3. From the results, all the methods consistently outperform Random under various levels of #MAdds. The multi-path AG consistently outperforms OFA-T at different levels of #MAdds. Our proposed single-path AG further outperforms the multi-path scheme by a large margin (89.43% vs. 88.73% at the budget level of 277M Avg. #MAdds), which demonstrates the effectiveness of the proposed architecture generator with the single-path architecture encoding. Compared with OFA-T, the multi-path AG has orders of magnitude lower training cost and search cost. More critically, our single-path AG further reduces the training cost, which demonstrates the efficiency of our single-path architecture generator in both training and architecture search. For example, our proposed architecture generator is able to generate architectures within 0.1 second for 50 development requirements.

## 5. Conclusion

In this paper, we have studied a new challenging problem of efficient deployment for different superclasses with various resources, where the superclass of interest and resource constraint are dynamically specified at testing time.



To this end, we have proposed a novel and general framework, called Elastic Architecture Search (EAS), to instantly specialize neural networks at runtime. The proposed EAS first trains an over-parameterized network with the **super-class dropout** strategy that randomly drops the output logits corresponding to different superclasses. In this way, the over-parameterized network supports many sub-networks for diverse superclasses once trained. Based on the well-trained over-parameterized network, we have further proposed an efficient architecture generator to instantly obtain architectures within a single forward pass given arbitrary superclasses and budgets during inference. Experiments on image classification datasets have shown the superiority of the proposed methods under diverse deployment scenarios.

## 6. Limitations and Future Work

The proposed EAS may bring some negative societal impacts, such as job losses for algorithm engineers. Moreover, improper uses of the proposed EAS may result in disastrous effects. For example, obtaining a very small network for an autonomous driving car may bring greater risks to the driver.

In the future, we may extend our method in three aspects. First, we currently perform neural architecture search based on the given specific superclass and budget. However, the superclass label is often unknown in many real-world applications. To address this, we will need to perform superclass prediction first and then use the proposed method to obtain architectures. Second, we may consider multiple superclasses at testing time, where different superclass combinations might have overlapped classes. This is a very challenging scenario due to the large combinatorial space. For example, for 100 superclasses, we have roughly  $2^{100}$  different superclass combinations. Third, we may extend our proposed method to broader applications, such as dense prediction, machine translation, *etc.*

## References

- [1] Rie Kubota Ando, Tong Zhang, and Peter Bartlett. A framework for learning predictive structures from multiple tasks and unlabeled data. *J. Mach. Learn. Res.*, pages 1817–1853, 2005. [3](#)
- [2] Yoshua Bengio, Nicholas Léonard, and Aaron Courville. Estimating or propagating gradients through stochastic neurons for conditional computation. *arXiv preprint arXiv:1308.3432*, 2013. [5](#)
- [3] Han Cai, Chuang Gan, Tianzhe Wang, Zhekai Zhang, and Song Han. Once-for-all: Train one network and specialize it for efficient deployment. In *Proc. Int. Conf. Learn. Repren.*, 2020. [2](#), [3](#), [4](#), [7](#), [8](#), [12](#), [14](#)
- [4] Han Cai, Ligeng Zhu, and Song Han. ProxylessNAS: Direct neural architecture search on target task and hardware. In *Proc. Int. Conf. Learn. Repren.*, 2019. [1](#), [2](#), [3](#)
- [5] Jianhui Chen, Ji Liu, and Jieping Ye. Learning incoherent sparse and low-rank patterns from multiple tasks. *ACM Trans. Knowl. Discov. Data*, pages 22:1–22:31, 2012. [3](#)
- [6] Jianhui Chen, Lei Tang, Jun Liu, and Jieping Ye. A convex formulation for learning shared structures from multiple tasks. In *Proc. Int. Conf. Mach. Learn.*, pages 137–144, 2009. [3](#)
- [7] Xin Chen, Lingxi Xie, Jun Wu, and Qi Tian. Progressive differentiable architecture search: Bridging the depth gap between search and evaluation. In *Proc. IEEE Int. Conf. Comp. Vis.*, pages 1294–1303, 2019. [1](#)
- [8] An-Chieh Cheng, Chieh Hubert Lin, Da-Cheng Juan, Wei Wei, and Min Sun. Instanas: Instance-aware neural architecture search. In *Proc. AAAI Conf. on Arti. Intel.*, pages 3577–3584, 2020. [3](#)
- [9] Koby Crammer and Yishay Mansour. Learning multiple tasks using shared hypotheses. In *Proc. Adv. Neural Inf. Process. Syst.*, pages 1484–1492, 2012. [3](#)
- [10] Jia Deng, Wei Dong, Richard Socher, Li-Jia Li, Kai Li, and Li Fei-Fei. Imagenet: A large-scale hierarchical image database. In *Proc. IEEE Conf. Comp. Vis. Patt. Recogn.*, pages 248–255, 2009. [6](#), [12](#)
- [11] Emily L Denton, Wojciech Zaremba, Joan Bruna, Yann LeCun, and Rob Fergus. Exploiting linear structure within convolutional networks for efficient evaluation. In *Proc. Adv. Neural Inf. Process. Syst.*, pages 1269–1277, 2014. [2](#)
- [12] Logan Engstrom, Andrew Ilyas, Shibani Santurkar, and Dimitris Tsipras. Robustness (python library), 2019. [6](#), [12](#)
- [13] Steven K. Esser, Jeffrey L. McKinstry, Deepika Bablani, Rathinakumar Appuswamy, and Dharmendra S. Modha. Learned step size quantization. In *Proc. Int. Conf. Learn. Repren.*, 2020. [2](#)
- [14] Theodoros Evgeniou and Massimiliano Pontil. Regularized multi-task learning. In *Proc. ACM SIGKDD Int. Conf. Knowl. Discov. Data Min.*, pages 109–117, 2004. [3](#)
- [15] Hehe Fan, Zhongwen Xu, Linchao Zhu, Chenggang Yan, Jianjun Ge, and Yi Yang. Watching a small portion could be as good as watching all: Towards efficient video classification. In *Proc. Int. Joint Conf. Artif. Intell.*, pages 705–711, 2018. [3](#)
- [16] Shaopeng Guo, Yujie Wang, Quanquan Li, and Junjie Yan. Dmcp: Differentiable markov channel pruning for neural networks. In *Proc. IEEE Conf. Comp. Vis. Patt. Recogn.*, pages 1536–1544, 2020. [2](#)
- [17] Yong Guo, Yafo Chen, Yin Zheng, Qi Chen, Peilin Zhao, Jian Chen, Junzhou Huang, and Mingkui Tan. Pareto-frontier-aware neural architecture generation for diverse budgets. *arXiv preprint arXiv:2103.00219*, 2021. [4](#)
- [18] Yong Guo, Yafo Chen, Yin Zheng, Peilin Zhao, Jian Chen, Junzhou Huang, and Mingkui Tan. Breaking the curse of space explosion: Towards efficient nas with curriculum search. In *Proc. Int. Conf. Mach. Learn.*, pages 3822–3831, 2020. [2](#)
- [19] Y. Guo, Y. Zheng, Mingkui Tan, Qi Chen, Jian Chen, P. Zhao, and J. Huang. Nat: Neural architecture transformer for accurate and compact architectures. In *Proc. Adv. Neural Inf. Process. Syst.*, pages 735–747, 2019. [4](#)
- [20] Zichao Guo, Xiangyu Zhang, Haoyuan Mu, Wen Heng, Zechun Liu, Yichen Wei, and Jian Sun. Single path one-shot neural architecture search with uniform sampling. In *Proc. Eur. Conf. Comp. Vis.*, pages 544–560, 2020. [2](#), [3](#)

- [21] Kaiming He, Xiangyu Zhang, Shaoqing Ren, and Jian Sun. Deep residual learning for image recognition. In *Proc. IEEE Conf. Comp. Vis. Patt. Recogn.*, pages 770–778, 2016. [1](#)
- [22] Geoffrey Hinton, Oriol Vinyals, and Jeff Dean. Distilling the knowledge in a neural network. *arXiv preprint arXiv:1503.02531*, 2015. [2](#), [12](#)
- [23] Geoffrey E. Hinton, Nitish Srivastava, Alex Krizhevsky, Ilya Sutskever, and Ruslan Salakhutdinov. Improving neural networks by preventing co-adaptation of feature detectors. *arXiv preprint arXiv:1207.0580*, 2012. [3](#)
- [24] Andrew Howard, Mark Sandler, Grace Chu, Liang-Chieh Chen, Bo Chen, Mingxing Tan, Weijun Wang, Yukun Zhu, Ruoming Pang, Vijay Vasudevan, et al. Searching for mobilenetv3. In *Proc. IEEE Int. Conf. Comp. Vis.*, pages 1314–1324, 2019. [7](#)
- [25] Andrew G Howard, Menglong Zhu, Bo Chen, Dmitry Kalenichenko, Weijun Wang, Tobias Weyand, Marco Andreetto, and Hartwig Adam. Mobilenets: Efficient convolutional neural networks for mobile vision applications. *arXiv preprint arXiv:1704.04861*, 2017. [1](#)
- [26] Gao Huang, Danlu Chen, Tianhong Li, Felix Wu, Laurens van der Maaten, and Kilian Q Weinberger. Multi-scale dense networks for resource efficient image classification. In *Proc. Int. Conf. Learn. Repr.*, 2018. [3](#)
- [27] Sian-Yao Huang and Wei-Ta Chu. Searching by generating: Flexible and efficient one-shot nas with architecture generator. In *Proc. IEEE Conf. Comp. Vis. Patt. Recogn.*, pages 983–992, 2021. [2](#)
- [28] Max Jaderberg, Andrea Vedaldi, and Andrew Zisserman. Speeding up convolutional neural networks with low rank expansions. In *Proc. Brit. Mach. Vis. Conf.*, 2014. [2](#)
- [29] Ali Jalali, Pradeep Ravikumar, Sujay Sanghavi, and Chao Ruan. A dirty model for multi-task learning. In *Proc. Adv. Neural Inf. Process. Syst.*, pages 964–972, 2010. [3](#)
- [30] Eric Jang, Shixiang Gu, and Ben Poole. Categorical reparameterization with gumbel-softmax. In *Proc. Int. Conf. Learn. Repr.*, 2017. [5](#)
- [31] Eunwoo Kim, Chanho Ahn, Philip HS Torr, and Songhwai Oh. Deep virtual networks for memory efficient inference of multiple tasks. In *Proc. IEEE Conf. Comp. Vis. Patt. Recogn.*, pages 2710–2719, 2019. [3](#)
- [32] Diederik P. Kingma and Jimmy Ba. Adam: A method for stochastic optimization. In *Proc. Int. Conf. Learn. Repr.*, 2015. [7](#)
- [33] Jonathan Krause, Michael Stark, Jia Deng, and Li Fei-Fei. 3d object representations for fine-grained categorization. In *Proc. IEEE Int. Conf. Comp. Vis. Workshops*, pages 554–561, 2013. [6](#)
- [34] Yuhang Li, Xin Dong, and Wei Wang. Additive powers-of-two quantization: An efficient non-uniform discretization for neural networks. In *Proc. Int. Conf. Learn. Repr.*, 2020. [2](#)
- [35] Yonggang Li, Guosheng Hu, Yongtao Wang, Timothy Hospedales, Neil M Robertson, and Yongxin Yang. Differentiable automatic data augmentation. In *Proc. Eur. Conf. Comp. Vis.*, pages 580–595, 2020. [5](#)
- [36] Ji Lin, Yongming Rao, Jiwen Lu, and Jie Zhou. Runtime neural pruning. In *Proc. Adv. Neural Inf. Process. Syst.*, pages 2181–2191, 2017. [3](#)
- [37] Hanxiao Liu, Karen Simonyan, and Yiming Yang. DARTS: differentiable architecture search. In *Proc. Int. Conf. Learn. Repr.*, 2019. [2](#), [3](#), [7](#), [8](#)
- [38] Jing Liu, Bohan Zhuang, Zhuangwei Zhuang, Yong Guo, Junzhou Huang, Jinhui Zhu, and Mingkui Tan. Discrimination-aware network pruning for deep model compression. *IEEE Trans. Pattern Anal. Mach. Intell.*, 2021. [2](#)
- [39] Wu Liu, Tao Mei, Yongdong Zhang, Cherry Che, and Jiebo Luo. Multi-task deep visual-semantic embedding for video thumbnail selection. In *Proc. IEEE Conf. Comp. Vis. Patt. Recogn.*, pages 3707–3715, 2015. [3](#)
- [40] Zhuang Liu, Mingjie Sun, Tinghui Zhou, Gao Huang, and Trevor Darrell. Rethinking the value of network pruning. In *Proc. Int. Conf. Learn. Repr.*, 2019. [2](#)
- [41] Ilya Loshchilov and Frank Hutter. SGDR: stochastic gradient descent with warm restarts. In *Proc. Int. Conf. Learn. Repr.*, 2017. [7](#), [12](#)
- [42] Zhichao Lu, Kalyanmoy Deb, Erik D. Goodman, Wolfgang Banzhaf, and Vishnu Naresh Boddeti. Nsganetv2: Evolutionary multi-objective surrogate-assisted neural architecture search. In *Proc. Eur. Conf. Comp. Vis.*, pages 35–51, 2020. [2](#)
- [43] Zhichao Lu, Ian Whalen, Vishnu Boddeti, Yashesh D. Dhebar, Kalyanmoy Deb, Erik D. Goodman, and Wolfgang Banzhaf. Nsga-net: neural architecture search using multi-objective genetic algorithm. In *Proc. Genetic Evol. Comp. Conf.*, pages 419–427, 2019. [2](#)
- [44] Chris J. Maddison, Andriy Mnih, and Yee Whye Teh. The concrete distribution: A continuous relaxation of discrete random variables. In *Proc. Int. Conf. Learn. Repr.*, 2017. [5](#)
- [45] Pavlo Molchanov, Stephen Tyree, Tero Karras, Timo Aila, and Jan Kautz. Pruning convolutional neural networks for resource efficient inference. In *Proc. Int. Conf. Learn. Repr.*, 2017. [1](#), [2](#)
- [46] Shibin Parameswaran and Kilian Q. Weinberger. Large margin multi-task metric learning. In *Proc. Adv. Neural Inf. Process. Syst.*, pages 1867–1875, 2010. [3](#)
- [47] Wonpyo Park, Dongju Kim, Yan Lu, and Minsu Cho. Relational knowledge distillation. In *Proc. IEEE Conf. Comp. Vis. Patt. Recogn.*, pages 3967–3976, 2019. [2](#)
- [48] Bo Peng, Wenming Tan, Zheyang Li, Shun Zhang, Di Xie, and Shiliang Pu. Extreme network compression via filter group approximation. In *Proc. Eur. Conf. Comp. Vis.*, pages 307–323, 2018. [2](#)
- [49] Hieu Pham, Melody Y. Guan, Barret Zoph, Quoc V. Le, and Jeff Dean. Efficient neural architecture search via parameter sharing. In *Proc. Int. Conf. Mach. Learn.*, pages 4092–4101, 2018. [2](#), [3](#), [4](#)
- [50] Ning Qian. On the momentum term in gradient descent learning algorithms. *Neural Netw.*, pages 145–151, 1999. [7](#), [12](#)
- [51] Alec Radford, Luke Metz, and Soumith Chintala. Unsupervised representation learning with deep convolutional generative adversarial networks. In *Proc. Int. Conf. Learn. Repr.*, 2016. [4](#)
- [52] Esteban Real, Alok Aggarwal, Yanping Huang, and Quoc V Le. Regularized evolution for image classifier architecture search. In *Proc. AAAI Conf. on Arti. Intel.*, pages 4780–4789, 2019. [2](#)

- [53] Esteban Real, Sherry Moore, Andrew Selle, Saurabh Saxena, Yutaka Leon Suematsu, Jie Tan, Quoc V Le, and Alexey Kurakin. Large-scale evolution of image classifiers. In *Proc. Int. Conf. Mach. Learn.*, pages 2902–2911, 2017. **2**
- [54] Adria Recasens, Petr Kellnhofer, Simon Stent, Wojciech Matusik, and Antonio Torralba. Learning to zoom: a saliency-based sampling layer for neural networks. In *Proc. Eur. Conf. Comp. Vis.*, pages 52–67, 2018. **3**
- [55] Mengye Ren, Andrei Pokrovsky, Bin Yang, and Raquel Urtasun. Sbnnet: Sparse blocks network for fast inference. In *Proc. IEEE Conf. Comp. Vis. Patt. Recogn.*, pages 8711–8720, 2018. **3**
- [56] Shaoqing Ren, Kaiming He, Ross B. Girshick, and Jian Sun. Faster R-CNN: towards real-time object detection with region proposal networks. *IEEE Trans. Pattern Anal. Mach. Intell.*, pages 1137–1149, 2017. **1**
- [57] Adriana Romero, Nicolas Ballas, Samira Ebrahimi Kahou, Antoine Chassang, Carlo Gatta, and Yoshua Bengio. Fitnets: Hints for thin deep nets. In *Proc. Int. Conf. Learn. Repr.*, 2015. **2**
- [58] Robin Ru, Pedro M. Esperança, and Fabio Maria Carlucci. Neural architecture generator optimization. In *Proc. Adv. Neural Inf. Process. Syst.*, 2020. **3**
- [59] Mark Sandler, Andrew Howard, Menglong Zhu, Andrey Zhmoginov, and Liang-Chieh Chen. Mobilenetv2: Inverted residuals and linear bottlenecks. In *Proc. IEEE Conf. Comp. Vis. Patt. Recogn.*, pages 4510–4520, 2018. **1, 7**
- [60] Dimitrios Stamoulis, Ruizhou Ding, Di Wang, Dimitrios Lymberopoulos, Bodhi Priyantha, Jie Liu, and Diana Marculescu. Single-path NAS: designing hardware-efficient convnets in less than 4 hours. In *Eur. Conf. Mach. Learn. Princ. Pract. Knowl. Discovery in Databases*, pages 481–497, 2019. **2**
- [61] Dimitrios Stamoulis, Ruizhou Ding, Di Wang, Dimitrios Lymberopoulos, Bodhi Priyantha, Jie Liu, and Diana Marculescu. Single-path mobile automl: Efficient convnet design and NAS hyperparameter optimization. *IEEE J. Sel. Top. Signal Process.*, pages 609–622, 2020. **2, 5**
- [62] Ximeng Sun, Rameswar Panda, Rogerio Feris, and Kate Saenko. Adashare: Learning what to share for efficient deep multi-task learning. In *Proc. Adv. Neural Inf. Process. Syst.*, volume 33, pages 8728–8740, 2020. **3**
- [63] Mingxing Tan, Bo Chen, Ruoming Pang, Vijay Vasudevan, Mark Sandler, Andrew Howard, and Quoc V. Le. Mnasnet: Platform-aware neural architecture search for mobile. In *Proc. IEEE Conf. Comp. Vis. Patt. Recogn.*, pages 2820–2828, 2019. **2**
- [64] Sebastian Thrun and Joseph O’Sullivan. Discovering structure in multiple learning tasks: The tc algorithm. In *Proc. Int. Conf. Mach. Learn.*, pages 489–497, 1996. **3**
- [65] Li Wan, Matthew D. Zeiler, Sixin Zhang, Yann LeCun, and Rob Fergus. Regularization of neural networks using drop-connect. In *Proc. Int. Conf. Mach. Learn.*, pages 1058–1066, 2013. **3**
- [66] Xin Wang, Fisher Yu, Zi-Yi Dou, Trevor Darrell, and Joseph E Gonzalez. Skipnet: Learning dynamic routing in convolutional networks. In *Proc. Eur. Conf. Comp. Vis.*, pages 420–436, 2018. **3**
- [67] Yulin Wang, Kangchen Lv, Rui Huang, Shiji Song, Le Yang, and Gao Huang. Glance and focus: a dynamic approach to reducing spatial redundancy in image classification. In *Proc. Adv. Neural Inf. Process. Syst.*, 2020. **3**
- [68] Bichen Wu, Xiaoliang Dai, Peizhao Zhang, Yanghan Wang, Fei Sun, Yiming Wu, Yuandong Tian, Peter Vajda, Yangqing Jia, and Kurt Keutzer. Fbnet: Hardware-aware efficient convnet design via differentiable neural architecture search. In *Proc. IEEE Conf. Comp. Vis. Patt. Recogn.*, pages 10734–10742, 2019. **2, 8**
- [69] Wenhao Wu, Dongliang He, Xiao Tan, Shifeng Chen, Yi Yang, and Shilei Wen. Dynamic inference: A new approach toward efficient video action recognition. In *Proc. IEEE Conf. Comp. Vis. Patt. Recogn. Workshops*, pages 2890–2898, 2020. **3**
- [70] Zuxuan Wu, Caiming Xiong, Yu-Gang Jiang, and Larry S Davis. Liteeval: A coarse-to-fine framework for resource efficient video recognition. In *Proc. Adv. Neural Inf. Process. Syst.*, pages 7778–7787, 2019. **3**
- [71] Saining Xie, Alexander Kirillov, Ross B. Girshick, and Kaiming He. Exploring randomly wired neural networks for image recognition. In *Proc. IEEE Int. Conf. Comp. Vis.*, pages 1284–1293, 2019. **3**
- [72] Jiahui Yu and Thomas S Huang. Universally slimmable networks and improved training techniques. In *Proc. IEEE Int. Conf. Comp. Vis.*, pages 1803–1811, 2019. **12**
- [73] Jiahui Yu, Pengchong Jin, Hanxiao Liu, Gabriel Bender, Pieter-Jan Kindermans, Mingxing Tan, Thomas Huang, Xiaodan Song, Ruoming Pang, and Quoc Le. Bignas: Scaling up neural architecture search with big single-stage models. In *Proc. Eur. Conf. Comp. Vis.*, pages 702–717, 2020. **2, 3, 4**
- [74] Xiyu Yu, Tongliang Liu, Xinchao Wang, and Dacheng Tao. On compressing deep models by low rank and sparse decomposition. In *Proc. IEEE Conf. Comp. Vis. Patt. Recogn.*, pages 67–76, 2017. **2**
- [75] Sergey Zagoruyko and Nikos Komodakis. Paying more attention to attention: Improving the performance of convolutional neural networks via attention transfer. In *Proc. Int. Conf. Learn. Repr.*, 2017. **2**
- [76] Zhanpeng Zhang, Ping Luo, Chen Change Loy, and Xiaoou Tang. Facial landmark detection by deep multi-task learning. In *Proc. Eur. Conf. Comp. Vis.*, pages 94–108, 2014. **3**
- [77] Shuchang Zhou, Yuxin Wu, Zekun Ni, Xinyu Zhou, He Wen, and Yuheng Zou. Dorefa-net: Training low bitwidth convolutional neural networks with low bitwidth gradients. *arXiv preprint arXiv:1606.06160*, 2016. **2, 5**
- [78] Bohan Zhuang, Chunhua Shen, Mingkui Tan, Lingqiao Liu, and Ian Reid. Towards effective low-bitwidth convolutional neural networks. In *Proc. IEEE Conf. Comp. Vis. Patt. Recogn.*, pages 7920–7928, 2018. **1, 2**
- [79] Zhuangwei Zhuang, Mingkui Tan, Bohan Zhuang, Jing Liu, Yong Guo, Qingyao Wu, Junzhou Huang, and Jinhui Zhu. Discrimination-aware channel pruning for deep neural networks. In *Proc. Adv. Neural Inf. Process. Syst.*, pages 883–894, 2018. **1**
- [80] Barret Zoph and Quoc V. Le. Neural architecture search with reinforcement learning. In *Proc. Int. Conf. Learn. Repr.*, 2017. **1, 2**

## Appendix

We organize our supplementary material as follows.

- In Section A, we provide more details about the datasets.
- In Section B, we describe more implementation details about the proposed method and baselines.
- In Section C, we show the results of different methods on Car-20 dataset.
- In Section D, we investigate the effect of different drop rates.
- In Section E, we include more results to investigate the effect of searching architectures for each superclass.
- In Section F, we show the visualization results of the searched architectures.

### A. More details about the datasets

In this section, we introduce more details about the datasets mentioned in Section 4. Based on ImageNet [10], we construct two datasets for different superclasses following [12], namely ImageNet-10 and ImageNet-12. Based on Stanford Cars, we construct Car-20. We show more details of ImageNet-10, ImageNet-12 and Car-20 in Tables A, B and C, respectively.

Table A. More details about ImageNet-10. We report the names of superclasses and classes in it. Each class name is separated by a comma.

Superclass	Class
Dog	Chihuahua, Japanese spaniel, Maltese dog, Pekinese, Shih-Tzu, Blenheim spaniel
Bird	Cock, Hen, Ostrich, Brambling, Goldfinch, House finch
Insect	Tiger beetle, Ladybug, Ground beetle, Long-horned beetle, Leaf beetle, Dung beetle
Monkey	Guenon, Patas, Baboon, Macaque, Langur, Colobus
Car	Jeep, Limousine, Cab, Beach wagon, Ambulance, Convertible
Cat	Leopard, Snow leopard, Jaguar, Lion, Cougar, Lynx
Truck	Tow truck, Moving van, Fire engine, Pickup, Garbage truck, Police van
Fruit	Granny Smith, Rapeseed, Corn, Acorn, Hip, Buckeye
Fungus	Agaric, Gyromitra, Stinkhorn, Earthstar, Hen-of-the-woods, Coral fungus
Boat	Gondola, Fireboat, Speedboat, Lifeboat, Yawl, Canoe

### B. More implementation details

In this section, we introduce more implementation details mentioned in Section 4. Following [3, 72], we use the knowledge distillation technique [22] to train the over-parameterized network. Specifically, we take the largest sub-network from the over-parameterized network as the teacher network. We train the teacher network for 120 epochs with a mini-batch size of 256. We use SGD with a momentum of 0.9 for optimization [50]. The weight decay is set to  $3 \times 10^{-5}$ . The learning rate starts at 0.1 and decays with cosine annealing [41]. We do not use the superclass dropout strategy during teacher training. For OFA-V and OFA-T, we first sample 16K sub-networks with different architectures and measure their accuracies of diverse superclasses on the validation set following [3]. We then train the accuracy predictor for 250 epochs using a mini-batch size of 256. We use SGD with momentum for optimization. The momentum term and weight decay are set to 0.9 and  $1 \times 10^{-4}$ , respectively. The learning rate is initialized to 0.1 and decreased to 0 following the cosine function.

### C. More results on Car-20

In this section, we provide more results on the fine-grained dataset Car-20. We show the results of different methods in Table D. For the average performance of all superclasses on different resource budgets, our EAS consistently outperforms OFA-T in terms of the model accuracy with comparable #MAdds. For example, our method surpasses OFA-T by 0.4% at the resource budget level of 377.8 M Avg. #MAdds. These results verify the effectiveness of our method.

Table B. More details about ImageNet-12. We report the names of superclasses and classes in it. Each class name is separated by a comma.

Superclass	Class
Dog	Chihuahua, Japanese spaniel, Maltese dog, Pekinese, Shih-Tzu, Blenheim spaniel, Papillon, Toy terrier, Rhodesian ridgeback, Afghan hound, Basset, Beagle, Bloodhound, Bluetick, Black-and-tan coonhound, Walker hound, English foxhound, Redbone, Borzoi, Irish wolfhound
Structure	Dam, Altar, Dock, Apiary, Bannister, Barbershop, Barn, Beacon, Boathouse, Bookshop, Brass, Breakwater, Butcher shop, Castle, Chainlink fence, Church, Cinema, Cliff dwelling, Coil, Confectionery
Bird	Cock, Hen, Ostrich, Brambling, Goldfinch, House finch, Junco, Indigo bunting, Robin, Bulbul, Jay, Magpie, Chickadee, Water ouzel, Kite, Bald eagle, Vulture, Great grey owl, African grey, Macaw
Clothing	Cowboy hat, Crash helmet, Abaya, Academic gown, Diaper, Apron, Feather boa, Football helmet, Bathing cap, Bearskin, Fur coat, Bikini, Gown, Bolo tie, Bonnet, Bow tie, Brassiere, Hoopskirt, Cardigan, Christmas stocking
Vehicle	Minivan, Model T, Ambulance, Amphibian, Electric locomotive, Fire engine, Barrow, Forklift, Beach wagon, Freight car, Garbage truck, Bicycle-built-for-two, Go-kart, Half track, Cab, Horse cart, Jeep, Jinrikisha, Limousine, Convertible
Reptile	Loggerhead, Leatherback turtle, Mud turtle, Terrapin, Box turtle, Banded gecko, Common iguana, American chameleon, Whiptail, Agama, Frilled lizard, Alligator lizard, Gila monster, Green lizard, African chameleon, Komodo dragon, African crocodile, American alligator, Triceratops, Thunder snake
Carnivore	Timber wolf, White wolf, Red wolf, Coyote, Dingo, Dhole, African hunting dog, Hyena, Red fox, Kit fox, Arctic fox, Grey fox, Cougar, Lynx, Leopard, Snow leopard, Jaguar, Lion, Tiger, Cheetah
Insect	Tiger beetle, Ladybug, Ground beetle, Long-horned beetle, Leaf beetle, Dung beetle, Rhinoceros beetle, Weevil, Fly, Bee, Ant, Grasshopper, Cricket, Walking stick, Cockroach, Mantis, Cicada, Leafhopper, Lacewing, Dragonfly
Instrument	Cornet, Maraca, Marimba, Accordion, Acoustic guitar, Drum, Electric guitar, Banjo, Oboe, Ocarina, Flute, Organ, Bassoon, French horn, Gong, Grand piano, Harmonica, Harp, Cello, Chime
Food	French loaf, Bagel, Pretzel, Head cabbage, Broccoli, Cauliflower, Zucchini, Spaghetti squash, Acorn squash, Butternut squash, Cucumber, Artichoke, Bell pepper, Cardoon, Mushroom, Strawberry, Orange, Lemon, Fig, Pineapple
Furniture	Cradle, Crib, Medicine chest, Desk, Dining table, Entertainment center, Barber chair, File, Bassinet, Folding chair, Four-poster, Studio couch, Park bench, Bookcase, Table lamp, Throne, Toilet seat, Chiffonier, China cabinet, Rocking chair
Primate	Indri, Orangutan, Gorilla, Chimpanzee, Gibbon, Siamang, Guenon, Patas, Baboon, Macaque, Langur, Colobus, Proboscis monkey, Marmoset, Capuchin, Howler monkey, Titi, Spider monkey, Squirrel monkey, Madagascar cat

## D. Effect of different drop rates

To investigate the effect of the superclass dropout strategy, we first train the over-parameterized networks with different drop rates  $q$  on ImageNet-10 and then use the proposed architecture generator to obtain architectures. We report the results in

Table C. More details about Car-20. We report the names of superclasses and classes in it. Each class name is separated by a comma.

Superclass	Class
Acura	Integra Type R 2001, TL Type-S 2008, ZDX Hatchback 2012
Aston Martin	V8 Vantage Coupe 2012, Virage Convertible 2012, Virage Coupe 2012
Audi	R8 Coupe 2012, S4 Sedan 2012, S5 Coupe 2012
Bentley	Arnage Sedan 2009, Continental Flying Spur Sedan 2007, Continental Supersports Conv. Convertible 2012
BMW	3 Series Sedan 2012, M6 Convertible 2010, Z4 Convertible 2012
Buick	Enclave SUV 2012, Rainier SUV 2007, Verano Sedan 2012
Chevrolet	Cobalt SS 2010, Silverado 1500 Classic Extended Cab 2007, TrailBlazer SS 2009
Chrysler	PT Cruiser Convertible 2008, Sebring Convertible 2010, Town and Country Minivan 2012
Dodge	Challenger SRT8 2011, Magnum Wagon 2008, Ram Pickup 3500 Quad Cab 2009
Ferrari	458 Italia Convertible 2012, Italia Coupe 2012, California Convertible 2012
Ford	F-450 Super Duty Crew Cab 2012, GT Coupe 2006, Mustang Convertible 2007
GMC	Acadia SUV 2012, Savana Van 2012, Terrain SUV 2012
Honda	Accord Sedan 2012, Odyssey Minivan 2007, Odyssey Minivan 2012
Hyundai	Accent Sedan 2012, Tucson SUV 2012, Veloster Hatchback 2012
Jeep	Grand Cherokee SUV 2012, Liberty SUV 2012, Wrangler SUV 2012
Lamborghini	Aventador Coupe 2012, Gallardo LP 570-4 Superleggera 2012, Reventon Coupe 2008
Mercedes-Benz	300-Class Convertible 1993, SL-Class Coupe 2009, Sprinter Van 2012
Nissan	Juke Hatchback 2012, Leaf Hatchback 2012, NV Passenger Van 2012
Suzuki	Aerio Sedan 2007, SX4 Hatchback 2012, SX4 Sedan 2012
Toyota	Camry Sedan 2012, Corolla Sedan 2012, Sequoia SUV 2012

Table D. Performance comparisons on Car-20. We report the Top-1 Accuracy (Acc.) of different architectures on diverse superclasses. “Avg. Acc.” and “Avg. #MAdds” denote the average Top-1 accuracy and the average number of multiply-adds, respectively.

Method	T-1	T-2	T-3	T-4	T-5	T-6	T-7	T-8	T-9	T-10	T-11	T-12	T-13	T-14	T-15	T-16	T-17	T-18	T-19	T-20	Avg. Acc. (%)	Avg. #MAdds (M)
OFA-T	97.6	87.5	84.7	95.1	95.8	98.3	100.0	100.0	100.0	80.8	99.2	99.3	96.7	88.0	97.0	88.6	100.0	100.0	81.7	94.4	94.2	227.0
EAS (Ours)	98.4	86.6	84.7	95.1	95.0	100.0	97.6	99.2	100.0	83.3	99.2	100.0	95.9	88.0	98.5	93.0	99.2	100.0	81.7	96.0	94.6	227.6
OFA-T	97.6	87.5	85.5	95.1	97.5	100.0	100.0	100.0	100.0	83.3	98.5	99.3	96.7	90.7	100.0	88.6	99.2	100.0	85.0	96.0	95.0	277.3
EAS (Ours)	99.2	87.5	87.9	92.7	95.0	99.2	100.0	100.0	100.0	85.0	99.2	100.0	97.5	88.9	100.0	91.2	100.0	100.0	85.0	95.2	95.2	277.5
OFA-T	97.6	88.4	87.9	95.1	98.3	99.2	100.0	100.0	100.0	83.3	99.2	100.0	95.9	91.7	100.0	88.6	100.0	100.0	84.2	96.0	95.3	326.0
EAS (Ours)	98.4	84.8	87.9	95.1	95.8	100.0	100.0	100.0	100.0	86.7	99.2	100.0	97.5	92.6	99.2	91.2	100.0	100.0	84.2	94.4	95.4	327.3
OFA-T	98.4	88.4	88.7	95.1	97.5	100.0	100.0	100.0	100.0	85.0	98.5	100.0	95.9	91.7	100.0	87.7	100.0	100.0	84.2	97.6	95.4	374.3
EAS (Ours)	99.2	87.5	87.9	96.7	96.6	99.2	100.0	100.0	100.0	85.0	99.2	100.0	95.9	94.4	100.0	92.1	100.0	100.0	85.0	96.8	95.8	377.8

Figure A. From the results, EAS with a drop rate of 0.6 achieves the best performance. For example, at the #MAdds level of 316 M, the Top-1 accuracy of the proposed EAS with a drop rate of 0.6 is 89.7%, which is higher than those with other drop rates. Hence, we set  $q$  to 0.6 by default in our experiments on ImageNet-10. Moreover, with the increase of  $q$ , the performance of the searched architectures first goes better and then goes worse. These results demonstrate the effectiveness of the proposed superclass dropout strategy.

### E. More results on the effectiveness of searching architectures for each superclass

To further investigate the effectiveness of searching architectures for each superclass, we first train the over-parameterized network with superclass dropout on ImageNet-10 and then use the following methods to search for architectures. **EAS-V**: we apply the proposed EAS to find a single architecture for all superclasses. **EAS**: we use the proposed EAS to find an architecture for each superclass. From Table E, finding a specific architecture for each superclass outperforms that of searching a single architecture for all superclasses. For example, at the average #MAdds level of 219 M, EAS outperforms EAS-V by 0.8% in terms of the average Top-1 accuracy. These results show the necessity of finding architectures for each superclass.

### F. Visualization of the searched architectures

To demonstrate the effectiveness of the proposed method, we first compute the cosine similarity for each pair of the architectures among different superclasses under the same #MAdds level on ImageNet-10. Here, we use the one-hot encoding to encode the architecture following [3]. We then compute the average cosine similarity for each #MAdds level and report the results in Figure B. From the results, the average cosine similarity first increases and then saturates with the increase of

Table E. Performance comparisons between EAS-V and EAS on ImageNet-10. EAS-V denotes that we apply the proposed EAS to find a single architecture for all superclasses. EAS indicates that we apply the proposed EAS to find an architecture for each superclass. We report the Top-1 Accuracy (Acc.) of different architectures on diverse superclasses. “T- $t$ ” indicates the  $t$ -th superclass. “Avg. Acc.” and “Avg. #MAdds” denote the average Top-1 accuracy and the average number of multiply-adds, respectively.

Method	T-1	T-2	T-3	T-4	T-5	T-6	T-7	T-8	T-9	T-10	Avg. Acc. (%)	Avg. #MAdds (M)
EAS-V	87.3	<b>91.3</b>	79.3	<b>81.3</b>	83.7	<b>88.7</b>	<b>86.7</b>	95.0	93.0	95.0	88.1	223
EAS (Ours)	<b>89.0</b>	<b>91.3</b>	<b>81.7</b>	<b>81.3</b>	<b>86.7</b>	<b>88.7</b>	83.0	<b>96.7</b>	<b>94.0</b>	<b>96.7</b>	<b>88.9</b>	<b>219</b>
EAS-V	88.0	91.3	<b>81.7</b>	79.0	84.7	<b>90.7</b>	82.3	96.3	93.7	<b>96.7</b>	88.4	274
EAS (Ours)	<b>90.0</b>	<b>92.0</b>	81.3	<b>80.3</b>	<b>87.7</b>	90.3	<b>84.3</b>	<b>97.3</b>	<b>94.3</b>	<b>96.7</b>	<b>89.4</b>	<b>269</b>
EAS-V	88.7	91.0	80.0	80.3	86.0	88.7	<b>84.7</b>	96.0	93.7	96.3	88.5	320
EAS (Ours)	<b>89.3</b>	<b>91.7</b>	<b>82.0</b>	<b>82.3</b>	<b>89.0</b>	<b>90.0</b>	84.3	<b>97.3</b>	<b>94.3</b>	<b>96.7</b>	<b>89.7</b>	<b>316</b>
EAS-V	<b>89.0</b>	91.3	81.7	80.0	87.0	88.0	82.7	95.3	94.3	96.7	88.6	374
EAS (Ours)	88.7	<b>91.7</b>	<b>82.0</b>	<b>82.3</b>	<b>88.7</b>	<b>90.3</b>	<b>85.3</b>	<b>97.3</b>	<b>95.0</b>	<b>97.3</b>	<b>89.9</b>	<b>361</b>

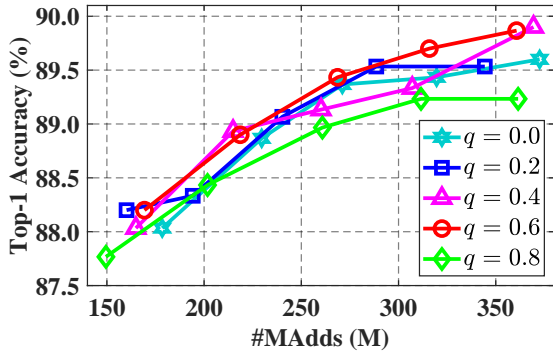


Figure A. Comparisons of the proposed EAS with different drop rates on ImageNet-10.

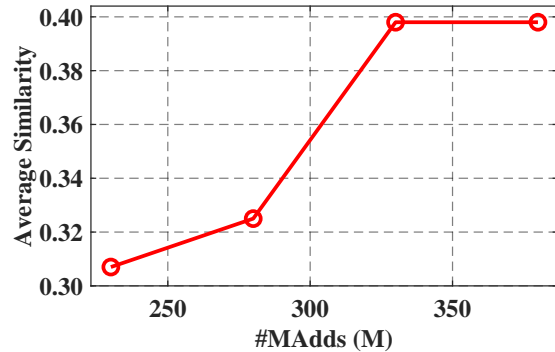


Figure B. The average architecture cosine similarity vs. #MAdds on ImageNet-10.

#MAdds. One possible reason is that the searched network tends to use larger kernel sizes, higher width expansion ratios, and more layers with the increase of #MAdds, which is shown in Figure C. Therefore, the searched architectures for different superclasses become more similar with the increase of #MAdds. We further show the searched architectures for different superclasses under the same level of #MAdds in Figure D. From the results, the searched architectures for different superclasses differ a lot, which demonstrates the motivation that the optimal architectures for diverse superclasses are different.

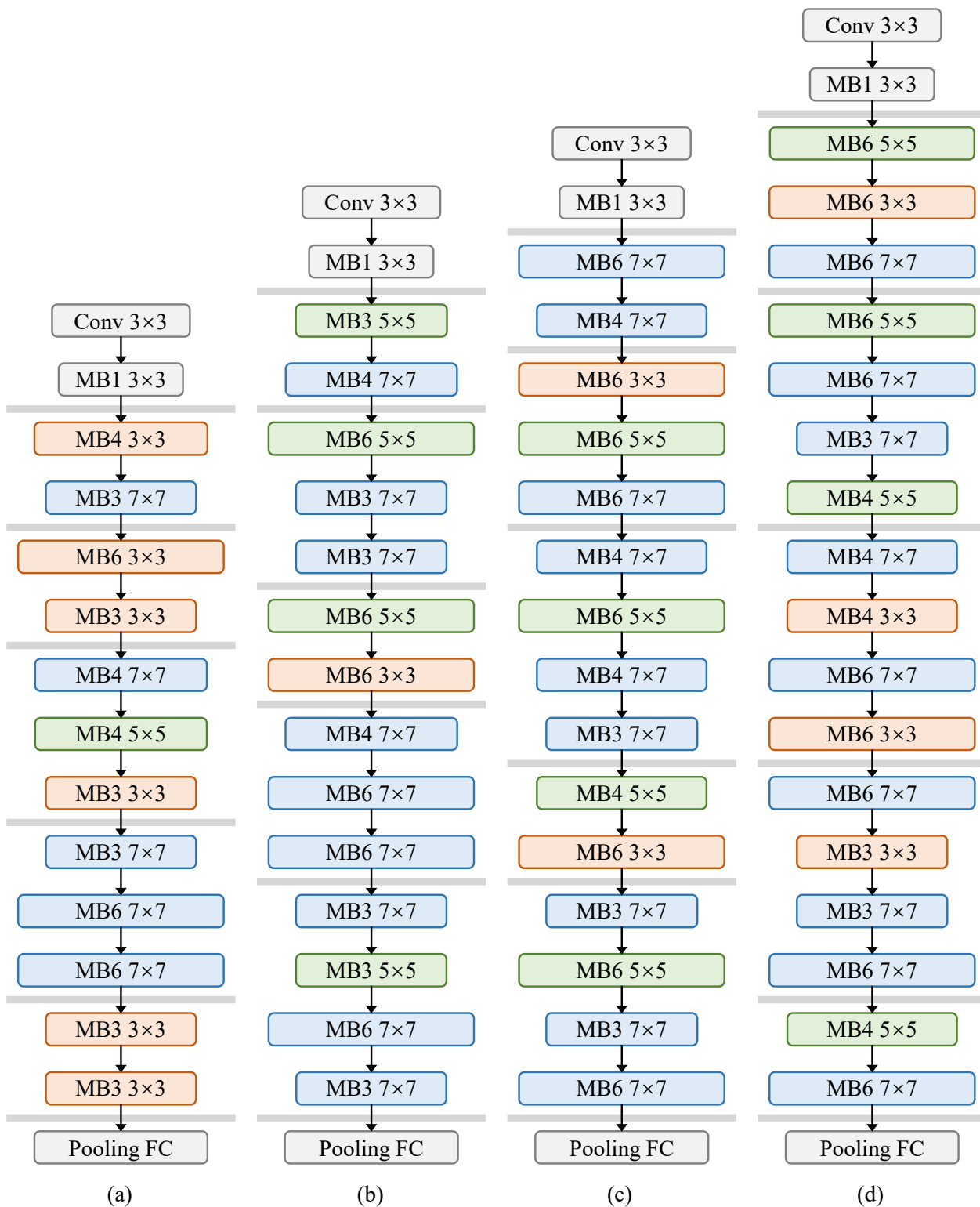


Figure C. The architectures searched by EAS for T-4 under various resource budgets on ImageNet-10. (a): The searched architecture at the #MAdds level of 219 M. (b): The searched architecture at the #MAdds level of 269 M. (c): The searched architecture at the #MAdds level of 316 M. (d): The searched architecture at the #MAdds level of 361 M.



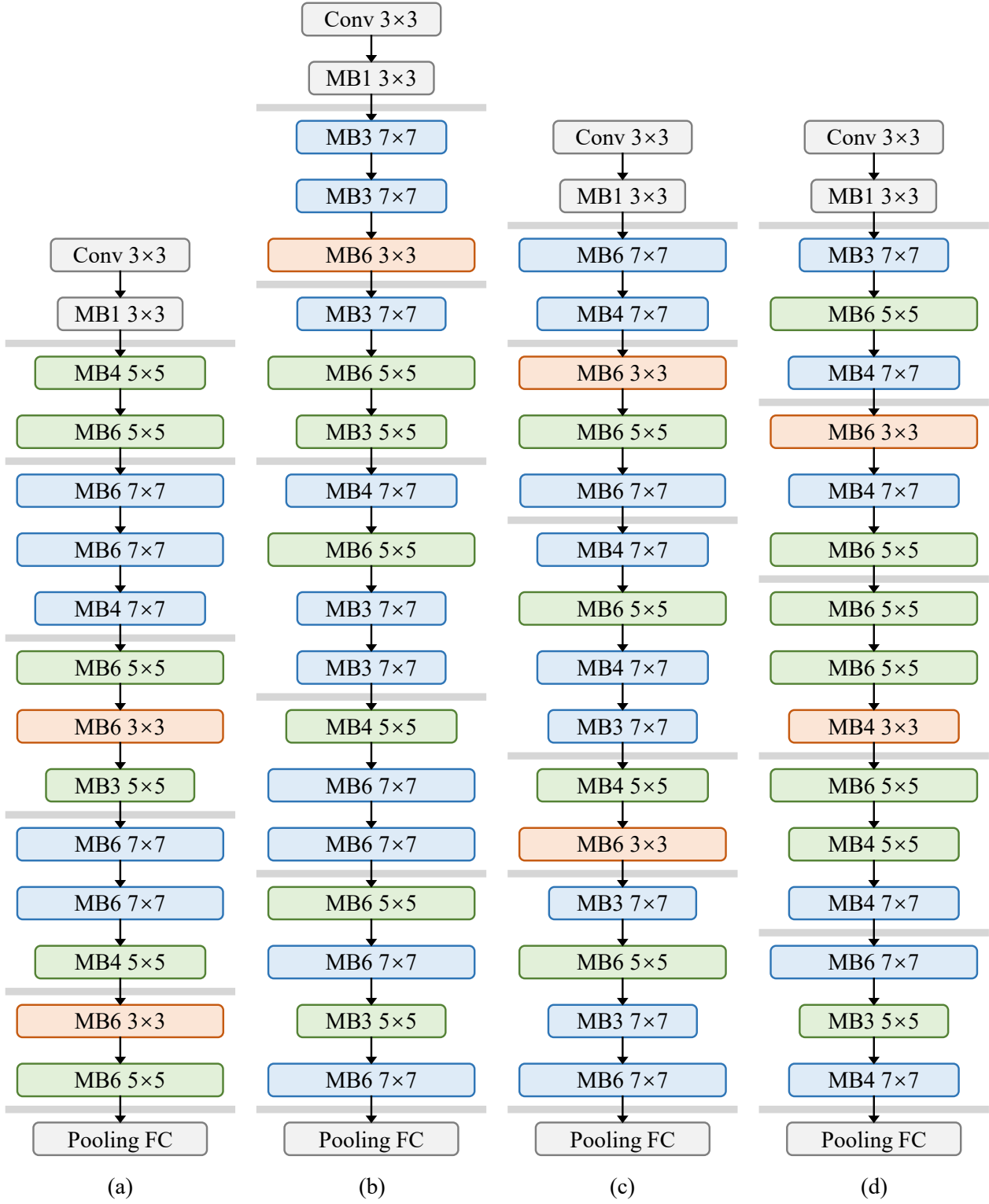


Figure D. The architectures searched by EAS at the #MAdds level of 316 M for different superclasses on ImageNet-10. (a): The searched architecture for T-1. (b) The searched architecture for T-3. (c): The searched architecture for T-4. (d): The searched architecture for T-7.